Intramolecular Photoinduced Electron Transfer to Anthraquinones Linked to Duplex DNA: The Effect of Gaps and Traps on Long-Range Radical Cation Migration

Susan M. Gasper and Gary B. Schuster*

Contribution from the School of Chemistry and Biochemistry, Georgia Institute of Technology, Atlanta, Georgia 30332

Received July 23, 1997[⊗]

Abstract: A series of duplex DNA structures was prepared that incorporate an anthraquinone group linked covalently to the 5′-terminus of one strand and two GG steps separated by three base pairs in the complementary strand. Physical, chemical, and spectroscopic methods indicate that the quinone is associated with the DNA by end-capping rather than by intercalation. Irradiation of the linked anthraquinone leads to piperidine-requiring strand cleavage predominantly at the 5′-G of the GG steps. The 5′-G of the distal GG step is more than 40 Å from the anthraquinone group. This long-range DNA damage is attributed to migration of a radical cation (hole) through the duplex DNA from its point of generation near the anthraquinone to its point of reaction at the GG step. This migration is not interrupted by imposition of a gap caused by an abasic site. However, the incorporation of 8-OxoG into the DNA duplex blocks migration by introducing a deep, reactive trap for the radical cation.

Introduction

The role played by DNA in molecular biology is clearly recognized to be vital to life on this planet. As the carrier of genetic information, DNA must preserve and transfer instructions precisely under appropriate control. It is for this reason that chemical damage to DNA can cause mutations.[1,2] Oxidation of DNA by free radicals,[3] ionizing radiation,[4,5] or photochemical means[6] is a common source of damage. Consequently, there has been immense interest in understanding the chemical and physical mechanisms that control the extent, location, and chemical consequences of DNA oxidation.[7−9] One manifestation of this interest is the attempt to understand the factors that control the efficiency and rate of the migration of oxidative damage in double-stranded DNA.[10] The motivation here is clear: migration of an oxidation event from its initial site in DNA to a sensitive, remote site will increase the efficiency of irreversible damage.

We recently discovered certain anthraquinone derivatives that intercalate in duplex DNA.[11] When the intercalated quinone is irradiated with UV light, it undergoes a relatively efficient electron transfer reaction that forms a quinone radical anion and a base radical cation.[12,13] This process results in oxidative damage that is revealed as strand breaks when the DNA is treated with piperidine. Although evidence indicates that the site of quinone intercalation is largely independent of base pair sequence,[11] the strand breaks occur predominantly at the 5′-G of GG steps. On the basis of these observations, we suggested a mechanism whereby a hole (base radical cation), formed initially by electron transfer to the excited quinone from a base at the intercalation site, "hops" through the duplex DNA until it is localized at a GG step where the radical cation reacts irreversibly with H_2O or O_2.[12,13] Support for this postulate comes from three sources: (i) laser spectroscopy, which clearly shows the rapid formation of the quinone radical anion,[11] (ii) detection of 7,8-dihydro-8-oxoguanine (8-OxoG), a characteristic guanine oxidation product,[12] and (iii) semiempirical calculations which indicate that GG steps may have a specially low oxidation potential.[14] However, since the location of the quinone on the DNA was not known unambiguously in these experiments, the hole-hopping mechanism remains somewhat speculative. Caution in this regard is especially prudent since it appears now that unsuspected cooperative binding to DNA can confound attempts to determine the mechanisms of hole and electron transport.[15,16]

We report herein an examination of anthraquinone derivatives that are linked covalently to DNA. Covalent attachment greatly restricts the allowable interaction geometries of the quinone with the DNA.[17−26] Irradiation of the linked quinone leads to strand

[⊗] Abstract published in *Advance ACS Abstracts,* December 15, 1997.

(1) Frenkel, K. *Pharmacol. Ther.* **1992**, *53*.
(2) Breen, A. P.; Murphy, J. A. *Free Radical Biol. Med.* **1995**, *18*, 1033−1077.
(3) Cheng, K. C.; Cahill, D. S.; Kasai, H.; Nishimura, S.; Loeb, L. A. *J. Biol. Chem.* **1992**, *267*.
(4) Boon, P. J.; Cullis, P. M.; Symons, M. C. R.; Wren, B. W. *J. Chem. Soc., Perkin Trans. 2* **1984**, 1393−1399.
(5) Wolf, P. G.; Jones, D. D.; Candeias, L. P.; O'Neill, P. *Int. J. Radiat. Biol.* **1993**, *64*, 7−18.
(6) Melvin, T.; Plumb, M. A.; Botchway, S. W.; O'Neill, P.; Parker, A. W. *Photochem. Photobiol.* **1995**, *61*, 584−591.
(7) Steenken, S. *Chem. Rev.* **1989**, *89*, 503.
(8) Cadet, J.; Vigny, P. *Bioorganic Photochemistry: Photochemistry and the Nucleic Acids*; John Wiley and Sons: New York, 1990; Vol. 1.
(9) Johnston, D. H.; Glasgow, K. C.; Thorp, H. H. *J. Am. Chem. Soc.* **1995**, *117*, 8993.
(10) O'Neill, P.; Fielden, E. M. *Adv. Radiat. Biol.* **1993**, *17*, 53−120.
(11) Armitage, B. A.; Yu, C.; Devadoss, C.; Schuster, G. B. *J. Am. Chem. Soc.* **1994**, *116*, 9847−9859.
(12) Ly, D.; Kan, Y.; Armitage, B.; Schuster, G. B. *J. Am. Chem. Soc.* **1996**, *118*, 8747−8748.
(13) Breslin, D. T.; Schuster, G. B. *J. Am. Chem. Soc.* **1996**, *118*, 2311−2319.
(14) Saito, I.; Takayama, M.; Sugiyama, H.; Nakatani, K.; Tsuchida, A.; Yamamoto, M. *J. Am. Chem. Soc.* **1995**, *117*, 6406−6407.
(15) Lincoln, P.; Tuite, E.; Norden, B. *J. Am. Chem. Soc.* **1997**, *119*, 1454−1455.
(16) Olson, E. J. C.; Hu, D.; Horman, A.; Barbara, P. F. *J. Phys. Chem. B* **1997**, *101*, 299−303.
(17) Orson, F. M.; Kinsey, B. M.; McShan, W. M. *Nucleic Acids Res.* **1994**, *22*, 479−484.
(18) Boutorine, A. S.; Tokuyama, H.; Takasugi, M.; Isobe, H.; Nakamura, E.; Helene, C. *Angew. Chem., Int. Ed. Engl.* **1994**, *33*, 2462−2465.
(19) Schubert, F.; Knaf, A.; Moller, U.; Chec, D. *Nucleosides Nucleotides* **1995**, *14*, 1437−1443.
(20) Meade, T. J.; Kayyem, J. F. *Angew. Chem., Int. Ed. Engl.* **1995**, *34*, 352−354.

S0002-7863(97)02496-7 CCC: $14.00

Chart 1

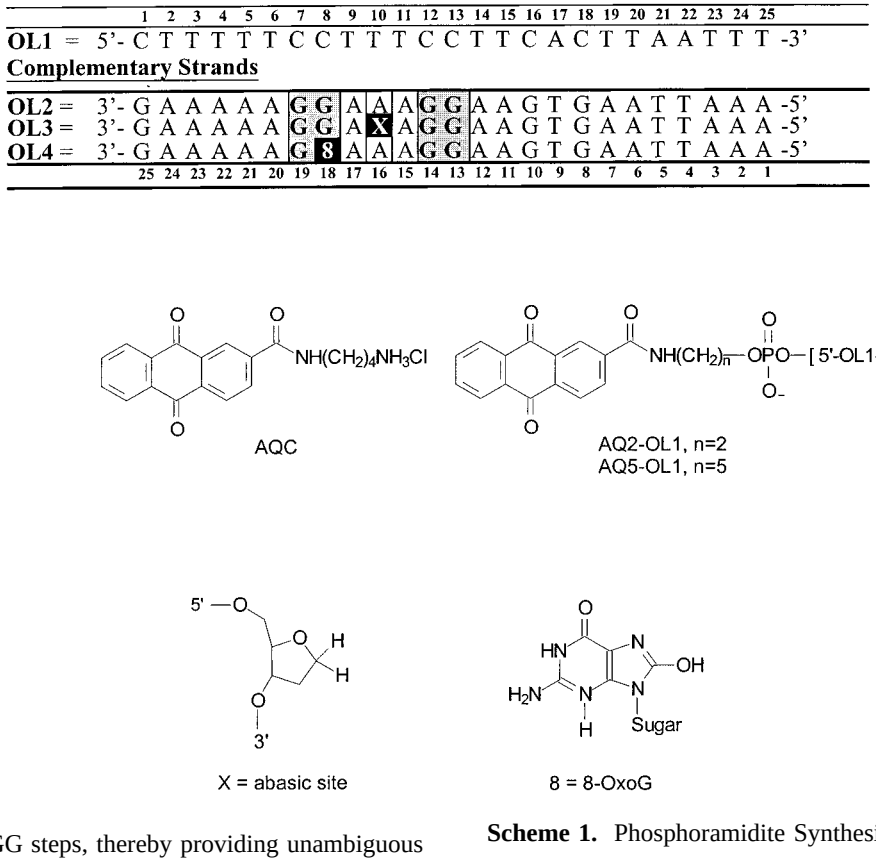

cleavage at remote GG steps, thereby providing unambiguous evidence that oxidative damage can migrate in double-stranded DNA. Examinations of the ability of the base radical cation to hop past traps and gaps reveals a robust process that is not easily interrupted. However, a deep trap (low oxidation potential site) is an effective blockade to further radical cation migration. These findings may have important implications to oxidative damage and repair mechanisms of genomic DNA.

Results

The two 25-base-containing oligonucleotides, shown in Chart 1, with anthraquinone derivatives covalently linked to the 5′-terminus were prepared. A series of oligonucleotides complementary to the anthraquinone-containing strand was also prepared. The duplexes formed with the complementary oligonucleotides were designed to address three questions concerning hole and electron transfer in double-stranded DNA: (i) Will the excited state of the covalently-linked quinone oxidize a base and introduce a radical cation into the duplex? (ii) Will that radical cation migrate from its site of introduction and initiate a chemical reaction at a remote site? (iii) What sort of trap or gap will slow or prevent migration of the radical cation? The experiments we report herein contribute to answering these questions and provide insight into the electron transport properties of duplex DNA.

Scheme 1. Phosphoramidite Synthesis

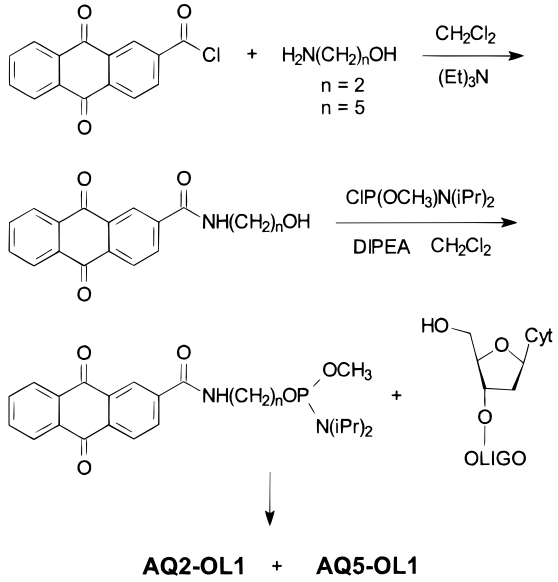

(1) Synthesis and Characterization of Anthraquinone−Oligonucleotide Conjugates. The **AQ5−OL1** and **AQ2−OL1** conjugates were prepared by automated solid-phase synthesis according to the method of Mori and co-workers.[27] The anthraquinone-derived phosphoramidites required for incorporation into the oligonucleotide were prepared as outlined in Scheme 1. Anthraquinone-2-carbonyl chloride was combined with either 2-amino-1-ethanol or 5-amino-1-pentanol to give *N*-(2-hydroxyethyl)- and *N*-(5-hydroxypentyl)-2-anthraquinonecarboxamides, respectively. These carboxamides were converted to phosphoramidites by reaction with *N*,*N*-diisopropylmethylphosphonamidic chloride. The phosphoramidites were

(21) Hall, D. B.; Holmlin, R. E.; Barton, J. K. *Nature* **1996**, *382*, 731−735.
(22) Dandliker, P. J.; Holmlin, R. E.; Barton, J. K. *Science* **1997**, *275*, 1465−1468.
(23) Mestre, B.; Jakobs, A.; Pratviel, G.; Meunier, B. *Biochemistry* **1996**, *35*, 9140−9149.
(24) Boutorine, A. S.; Brault, D.; Takasugi, M.; Delgado, O.; Helene, C. *J. Am. Chem. Soc*. **1996**, *118*, 9469−9476.
(25) Fukui, K.; Morimoto, M.; Segawa, H.; Tanaka, K.; Shimidzu, T. *Bioconjugate Chem*. **1996**, *7*, 349−355.
(26) Arkin, M. R.; Stemp, E. D.; Pulver, S. C.; Barton, J. K. *Chem. Biol*. **1997**, *4*, 389−400.
(27) Mori, K.; Subasinghe, C.; Cohen, J. S. *FEBS Lett*. **1989** *249*, 213−218.

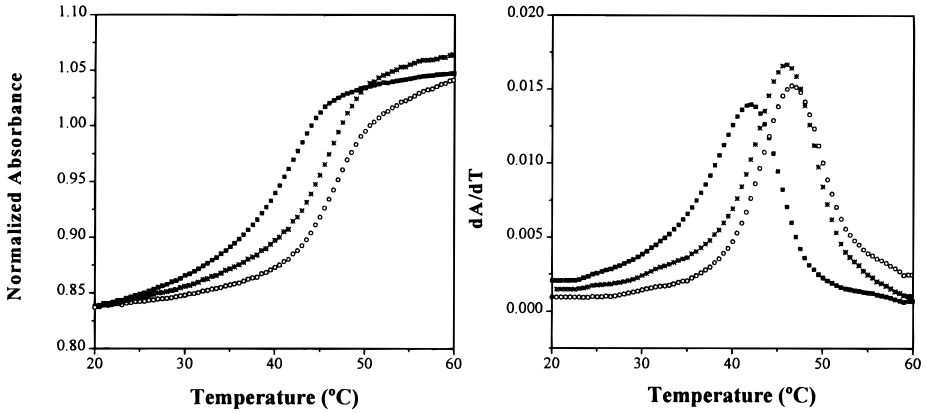

Figure 1. Cooling curves obtained by monitoring the absorbance of the 8-OxoG duplexes at 260 nm with decreasing temperature are shown on the left. The corresponding first-derivative curves are shown on the right: ■ = **OL1/OL4** duplex with T_m = 41.9 °C; ○ = **AQ2−OL1/OL4** duplex with T_m = 46.7 °C; * = **AQ5−OL1/OL4** duplex with T_m = 45.9 °C.

Table 1. HPLC Retention and Purity Data for DNA and Anthraquinone-Conjugated Oligonucleotides

sample	retn time (min)	% total area[a]
OL1	28.8	95.0
AQ2−OL1	30.0	98.5
AQ5−OL1	30.7	99.0

[a] Percentage of integrated area of the entire chromatogram contributed by the identified compound.

purified by column chromatography, characterized by ^{1}H and ^{31}P NMR spectroscopy, and coupled to the 5′-OH termini of the nascent oligonucleotides as the final step in the solid phase synthesis. The anthraquinone−oligonucleotide conjugate was deprotected, cleaved from the solid support following the standard procedure, desalted, and then purified by preparative scale HPLC. Details of the preparations are reported in the Experimental Section.

The **AQ2−OL1** and **AQ5−OL1** conjugates were characterized using matrix-assisted laser desorption ionization−time of flight (MALDI-TOF) mass spectrometry. The expected mass of **AQ2−OL1** is 7823.07 and a sharp peak in its spectrum is observed for a singly charged species at 7822.25. A second peak, for doubly charged **AQ2−OL1**, is observed at 3910.51. Similarly, the expected mass of **AQ5−OL1** is 7865.09 and MALDI-TOF peaks are observed at (*m*/*e*) = 7864.94 and 3929.15. These conjugates were also characterized by their UV absorption spectra and by reversed phase HPLC. The UV spectra of aqueous solutions of either **AQ2−OL1** or **AQ5−OL1** show a very strong absorbance band with a maximum at 260 nm and a weaker band in the 300−350 nm region. The peak at 260 nm is due to a combination of absorbances from chromophores in both the DNA and the anthraquinone portions of the structure. The absorbance measured in the 300−350 nm region is due solely to the anthraquinone chromophore. HPLC analyses of **AQ2−OL1**, **AQ5−OL1**, and the parent oligonucleotide, **OL1**, show only one peak for each compound, which confirms the purity of the preparation. The single peaks detected for **AQ2−OL1** and **AQ5−OL1** have absorption bands both at 260 nm and in the range 300−350 nm. The peak observed for **OL1** has only the 260 nm absorption. This observation confirms the covalent linkage of the anthraquinone chromophore to the oligonucleotide. Finally, the data in Table 1 show that the retention times for **AQ2−OL1** and **AQ5−OL1** increase as expected with increasing linker length.

(2) Hybrids of AQ2−OL1 and AQ5−OL1 with Complementary DNA: The Melting Behavior of the Duplexes. Duplex DNA was prepared by mixing equimolar amounts of conjugates **AQ2−OL1** or **AQ5−OL1** with their complementary DNA strands, **OL2**, **OL3**, or **OL4**, in phosphate-buffered solution. The mixtures was heated to ca. 80 °C and then cooled slowly to room temperature. The duplexes formed by this hybridization procedure were characterized by their melting behavior monitored by UV spectroscopy.

Table 2. T_m Data (°C) Obtained from First-Derivative Plots for Duplex DNA Conjugates

	OL2	**OL3**	**OL4**
AQ2−OL1	46.8	38.8	46.7
AQ5−OL1	46.6	37.9	45.9
OL1	41.3	33.7	41.9

The absorbance at 260 nm of the duplex DNA samples was monitored as the temperature was cycled from ca. 20 to 65 °C and then back to 20 °C. The cooling curves obtained for the 8-OxoG duplexes are shown in Figure 1. Each of the duplex structures studied in this work gives a similar curve. This melting behavior is typical of short oligonucleotides showing a single transition. The melting temperature (T_m) for **AQ2−OL1/OL2** was determined to be 46.8 °C from a first-derivative plot of the absorption data. The melting data for the oligonucleotides studied in this work are summarized in Table 2.

Surprisingly, the T_m of **AQ5−OL1/OL2** is essentially identical to that of **AQ2−OL1/OL2**. We had expected a higher T_m for **AQ5−OL1** because the longer linking chain can permit intercalation of the anthraquinone in the oligonucleotide.[23] Critically, the T_m of both **AQ2−OL1/OL2** and **AQ5−OL1/OL2** is ca. 5.4 °C higher than that observed for duplex **OL1/OL2**, which does not have a covalently linked anthraquinone group, indicating that the quinone is stabilizing both duplex structures. As expected, duplex **AQ2−OL1/OL3**, which has a dehydroxylated abasic residue[28] at position 16 of **OL3** (see Chart 1), has a T_m ca. 8 °C below that of **AQ2−OL1/OL2**.[29] This reflects the loss of hydrogen bond stabilization at the abasic site. On the other hand, the T_m for the duplex formed from **AQ2−OL1/OL4**, which has an 8-OxoG at position 18 of **OL3** (see Chart 1), is comparable with that of **AQ2−OL1/OL2**. This observation suggests that substitution of 8-OxoG for G has little impact on the stability of the duplex DNA.

(3) Phosphorescence of the Anthraquinone-Linked Duplexes. Previous examinations of anthraquinones related to **AQ2** and **AQ5** showed that their phosphorescence emission is nearly completely quenched when they are intercalated in duplex DNA.[13] In contrast, nonintercalative binding of a related

(28) Kalnik, M. W.; Chang, C. N.; Grollman, A. P.; Patel, D. J. *Biochemistry* **1988**, *27*, 924−931.
(29) Loeb, L. A.; Preston, B. D. *Annu. Rev. Genet.* **1986**, *20*, 201−230.

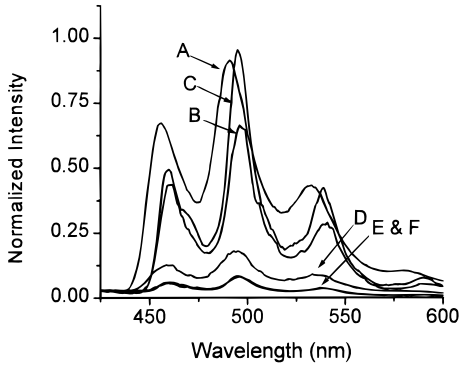

Figure 2. Anthraquinone phosphorescence emission spectra obtained from solutions of the appropriate anthraquinone derivative in 1:2 buffer: ethylene glycol at 77 K: A, free **AQC**; B, **AQ2**−**OL1**; C, **AQ5**−**OL1**; D, 10 μM **AQC** in the presence of **OL1/OL2**; E, **AQ2**−**OL1/OL2**; F, **AQ5**−**OL1/OL2**. The spectra obtained for E and F overlap.

quinone to DNA leads to much less efficient phosphorescence quenching.[30] The phosphorescence of duplexes **AQ2**−**OL1/OL2** and **AQ5**−**OL1/OL2** was investigated to assess further the association of the quinone with the DNA.

The phosphorescence emission spectra from single-stranded **AQ2**−**OL1**, **AQ5**−**OL1**, and their duplexes with **OL2** were compared with the emission of **AQC** (Chart 1), which we take as the standard. Each of these spectra was recorded in a 2:1 phosphate buffer:ethylene glycol solution at 77 K. Compared with **AQC** in the absence of DNA, single-stranded **AQ2**−**OL1** and **AQ5**−**OL1** exhibit only 45% and 29%, respectively, of the integrated emission intensity of the standard (Figure 2). This reduction in phosphorescence intensity signifies some contact between the quinone and the DNA bases in the coiled structure of the single-stranded DNA. Significantly, the phosphorescence intensity detected for both duplex **AQ2**−**OL1/OL2** and **AQ5**−**OL1/OL2** is reduced to less than 3% of that seen for free **AQC**. This finding clearly demonstrates that formation of the duplex structure enforces close association between the anthraquinone group and the bases of the DNA. This type of association is normally attributed to intercalative binding, but the linkage in **AQ2**−**OL1** appears from models to be too short to permit intercalation.

(4) Photoinduced Cleavage of Duplexes AQ2−**OL1/OL2 and AQ5**−**OL1/OL2.** Anthraquinone derivatives such as **AQC** give selective, UV light-induced cleavage of DNA. Irradiation of **AQC**, randomly intercalated in DNA, leads to alkali-dependent cleavage predominately at the 5′-G of GG steps with lesser amounts of cleavage at the 3′-G of this step and at the G of 3′-AG-5′ sequences.[11] Previous work has revealed this process to be initiated by electron transfer from a DNA base to the excited triplet state of the quinone followed by localization and reaction of the radical cation (hole) at the reactive G.[12,13] The covalent linkage of the anthraquinone in **AQ2**−**OL1** and **AQ5**−**OL1** prohibits direct contact with the GG steps of the complementary strand in duplexes formed with **OL2**, **OL3**, or **OL4**. We examined the photoinduced cleavage of these duplexes by polyacrylamide gel electrophoresis (PAGE) using complementary oligonucleotides that had been radiolabeled at the 5′-end with ^{32}P.

Irradiation of either **AQ2**−**OL1/OL2** or **AQ5**−**OL1/OL2** in phosphate buffer solution at 350 nm, where only the anthraquinone chromophore absorbs light, leads to piperidine-requiring cleavage in **OL2** at the GG steps at positions 13,14

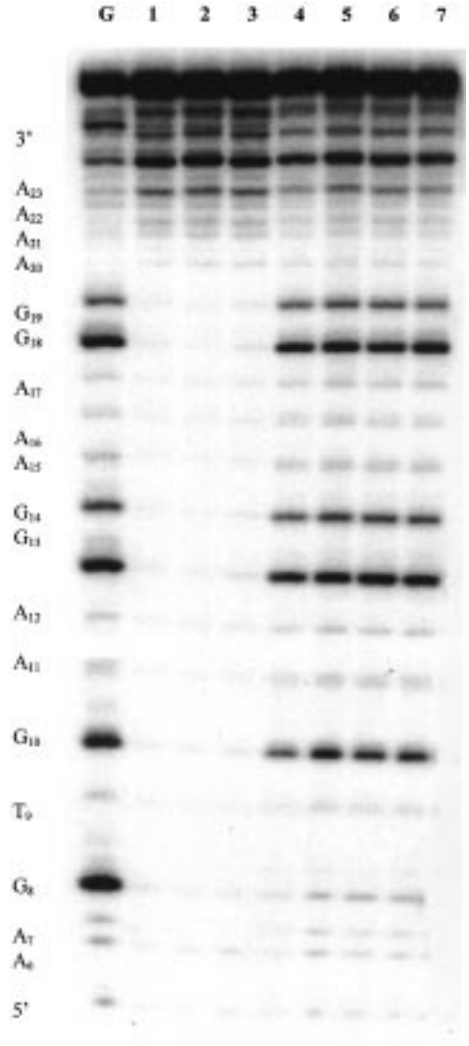

Figure 3. Autoradiogram demonstrating DNA cleavage of **OL2** in **AQ2**−**OL1/OL2** and **AQ5**−**OL1/OL2** duplexes as induced by irradiation of the anthraquinone (350 nm). Samples contained 5 μM duplex DNA and 4000 cpm ^{32}P end-labeled **OL2** in 10 mM sodium phosphate buffer (pH = 7). All samples are piperidine-treated. Control lanes (lanes 1−3): 1, 50 min irradiation of **OL1/OL2**; 2, 0 min irradiation of **AQ2**−**OL1/OL2**; 3, 50 min irradiation of 5 μM **AQC** in the presence of **OL1/OL2**. Anthraquinone irradiation (lanes 4−7): 4, 25 min irradiation of **AQ2**−**OL1/OL2**; 5, 50 min irradiation of **AQ2**−**OL1/OL2**; 6, 25 min irradiation of **AQ5**−**OL1/OL2**; 7, 50 min irradiation of **AQ5**−**OL1/OL2**. Cleavage products were separated on a 20% denaturing polyacrylamide gel. Lane G is the sequencing lane.

and 18,19 and at G_{10}, which is 5′ to an A (lanes 4−7 in Figure 3). In both cases the 5′-G is cleaved more efficiently than the 3′-G of the GG sequence. Significantly, both the proximal (18,-19) and distal (13,14) GG steps are cleaved with approximately the same overall efficiency. This behavior mimics that observed for **AQC** when it is randomly intercalated in duplex DNA.

In a control experiment, the irradiation of either **AQ2**−**OL1** or **AQ5**−**OL1** in the presence of a noncomplementary radiolabeled duplex containing three GG sites shows no cleavage (data not shown). In a second control experiment, a sample containing **OL1/OL2** (5 μM) and free **AQC** (5 μM) was irradiated. Again, no cleavage of the DNA is observed (Figure 3, lane 3). These control experiments confirm that the light-initiated reactions of **AQ2**−**OL1/OL2** and **AQ5**−**OL1/OL2** leading to the GG damage are intramolecular. In a third control experiment, we showed that the light-induced cleavage is not

(30) Breslin, D. T.; Coury, J. E.; Anderson, J. R.; McFail-Isom, L.; Kan, Y.; Williams, L. D.; Bottomley, L. A.; Schuster, G. B. *J. Am. Chem. Soc.* **1997**, *119*, 5043−5044.

inhibited when superoxide dismutase and catalase are added to the reaction mixture. This finding excludes a role for the hydroxyl radical in this process.[31,32]

Clearly, irradiation of these anthraquinone-conjugated duplexes causes a reaction on the complementary strand at great distance from the quinone location. This finding requires that some species capable of damaging guanine migrate from the quinone location to the GG sites. The migrating species could be a base radical cation transmitted from the quinone through the DNA, or it could be singlet oxygen ($^1O_2$). Both base radical cations and $^1O_2$ damage DNA at guanines.[33−35] We carried out a series of experiments to distinguish between these two possibilities.

The lifetime of $^1O_2$ increases ca. 10-fold when the reaction solvent is changed from H_2O to D_2O.[36] This effect has been used to verify the participation of $^1O_2$ in reactions with DNA since the increase in lifetime is manifested as a more efficient reaction.[37] We compared the efficiency of cleavage obtained by irradiation of **AQ2**−**OL1/OL2** and **AQ5**−**OL1/OL2** in H_2O and in D_2O. There is no measurable effect of the solvent change in either conjugated system. As a control experiment, the methylene blue (MB) sensitized reaction (a known source of $^1O_2$) of **AQ2**−**OL1/OL2** was studied in H_2O and D_2O. In this case there is a significant increase in cleavage efficiency in D_2O solution. These results confirm, at least, that the damage observed at the GG steps from irradiation of **AQ2**−**OL1/OL2** and **AQ5**−**OL1/OL2** is intramolecular. The H_2O/D_2O study eliminates freely diffusing $^1O_2$ as the reagent causing the long-range damage. However, Hèléne and co-workers have recently suggested that $^1O_2$ generated from a linked sensitizer may be capable of one-dimensional diffusion through a groove of DNA and thereby cause long-range reaction but not exhibit an isotope effect.[38] This possibility can be eliminated in the present case by comparison of the cleavage pattern obtained from the anthraquinone and MB-initiated reactions (Figure 4). In the latter, G_{10} and G_8 are cleaved with approximately equal efficiency. In the former, G_{10} is cleaved with much greater efficiency than G_8. Consequently, the agent responsible for the long-range damage in **AQ2**−**OL1/OL2** and **AQ5**−**OL1/OL2l** cannot be $^1O_2$. The reactive species is therefore assigned to a radical cation that migrates through the duplex DNA to the GG sites.

Previously reported experiments reveal that the excited state of **AQC** is reduced to its radical anion is less than 20 ps when it is intercalated in duplex DNA.[11] Such rapid reaction precludes quenching of the anthraquinone excited state by external reagents. Modeling indicates that the quinone may intercalate in **AQ5**−**OL1/OL2** but not in **AQ2**−**OL1/OL2**.[39,40] Therefore,

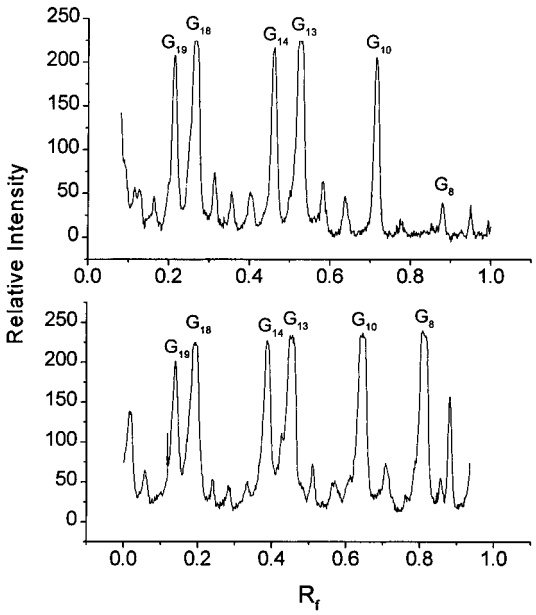

Figure 4. Histograms obtained by scanning autoradiogram comparing cleavage of **OL2** by **AQ2**−**OL1** and methylene blue. Upper plot: Cleavage band intensity for a sample of 5 μM **AQ2**−**OL1/OL2** in D_2O containing 10 mM phosphate irradiated at 350 nm followed by piperidine treatment. Lower plot: Cleavage band intensity for a sample containing 5 μM **AQ2**−**OL1/OL2** and 10 μM methylene blue in D_2O containing 10 mM phosphate irradiated at >600 nm followed by piperidine treatment.

at least for the latter case, the excited quinone may be susceptible to external quenchers.

Foote and co-workers recently reported the rate constants for total quenching of $^1O_2$ by nucleoside derivatives.[41] The adenosine derivative quenches $^1O_2$ more than 100 times slower than the guanosine derivative. But both adenine and guanine will quench the triplet state of anthraquinone at the diffusion-limited rate.[42] We examined the ability of deoxyadenosine monophosphate (dAMP) to quench the GG cleavage induced by irradiation of **AQ2**−**OL1/OL2**, **AQ5**−**OL1/OL2**, or **AQC**. Since dAMP bears negative charge, it will not associate with DNA. To quench the reaction, the excited quinone must be accessible from solution by this large reagent. Irradiation of either **AQ2**−**OL1/OL2** or **AQ5**−**OL1/OL2** in the presence of 100 mM dAMP results in significant quenching of the GG cleavage. This is not an effect of increased ionic strength since an equivalent amount of $NaClO_4$ does not inhibit the cleavage reaction. The ratio of G cleavage in the samples containing $NaClO_4$ to those containing dAMP as a quencher is 1.3 and 2.2 for **AQ2**−**OL1/OL2** and **AQ5**−**OL1/OL2**, respectively. In contrast, addition of 50 mM dAMP to a DNA solution containing **AQC** does not result in quenching. In fact, when compared with an equivalent amount of $NaClO_4$, cleavage by **AQC** is more efficient when dAMP is present. Since **AQC** is not covalently bound to the DNA, its cleavage efficiency is strongly concentration and ionic strength dependent because these parameters affect the amount that is bound. These quenching results make it clear that the quinone triplet states in **AQ5**−**OL1/OL2** and **AQ5**−**OL1/OL2** are accessible to anionic quenchers and the intercalated triplet state of **AQC** is not.

(5) A Gap (Abasic Site) on the Labeled Strand. Radical cation (hole) migration through DNA is most likely to occur

(31) Hertzberg, R. P.; Dervan, P. B. *J. Am. Chem. Soc.* **1982**, *102*, 313−315.

(32) The inclusion of catalase, with or without SOD, causes an increase in the observed piperidine-dependent cleavage quantum efficiency without any change in the cleavage pattern.

(33) Floyd, R. A.; West, M. S.; Eneff, K. L.; Schneider, J. E. *Arch. Biochem. Biophys.* **1989**, *273*, 106−111.

(34) Schneider, J. E.; Price, S.; Maidt, L.; Gutteridge, J. M. C.; Floyd, R. A. *Nucleic Acids Res.* **1990**, *18*, 631−635.

(35) Devasagayam, T. P. A.; Steenken, S.; Obendorf, M. S. W.; Schulz, W. A.; Sies, H. *Biochemistry* **1991**, *30*, 6283−6289.

(36) Rogers, M. A. J.; Snowden, P. T. *J. Am. Chem. Soc.* **1982**, *104*, 5541−5543.

(37) Showen, K. B.; Showen, R. L. *Solvent Isotope Effects on Enzyme Systems*; Academic Press: New York, 1982; Vol. 87.

(38) Boutorine, A. S.; Brault, D.; Takasugi, M.; Delgado, O.; Hélène, C. *J. Am. Chem. Soc.* **1996**, *118*, 9469−9476.

(39) Veal, J. M.; Wilson, W. D. *J. Biomol. Struct. Dyn.* **1991**, *8*, 1119−1145.

(40) Private communication with Professor Wilson of Georgia State University.

(41) Pratt, F.; Hou, C.-C.; Foote, C. S. *J. Am. Chem. Soc.* **1997**, *119*, 5051−5052.

(42) Steenken, S.; Jovanovic, S. V. *J. Am. Chem. Soc.* **1997**, *119*, 617−618.

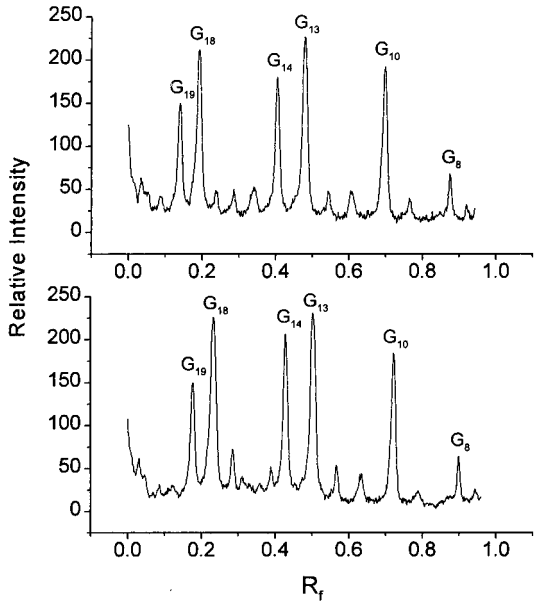

Figure 5. Histograms obtained by scanning autoradiogram comparing cleavage of **OL2** and **OL3** by **AQ5**−**OL1**. Upper plot: Cleavage band intensity for a sample of 5 μM **AQ5**−**OL1/OL2** in 10 mM phosphate irradiated at 350 nm followed by piperidine treatment. Lower plot: Cleavage band intensity for a sample containing 5 μM **AQ5**−**OL1/OL3** and in 10 mM phosphate irradiated at 350 nm followed by piperidine treatment. Similar data were obtained for the corresponding **AQ2**−**OL1** duplexes.

by overlap of the π-electrons of one base with those of an adjacent base along the strand.[43] Interruption of that overlap might lead to a measurable reduction in the ability of the hole to migrate to locations beyond the interruption. We prepared duplex **AQ2**−**OL1/OL3** and **AQ5**−**OL1/OL3** to address this question. The A_{16} of **OL2** is replaced by an abasic site in **OL3**. An abasic site contains the sugar−phosphate backbone of normal DNA, but the nucleobase at the 1-position of the deoxyribose is replaced by a hydrogen atom. This substitution is expected to introduce a gap, or a partial gap (see Discussion), in the π-electron overlap in that strand.

The A_{16} site in **OL2** is in between the proximal and the distal GG steps on that strand. Placement of the abasic site at this location in **OL3** provides an internal control for the efficiency of cleavage since, as a first assumption, the proximal GG should be unaffected by this change. Irradiation and analysis of **AQ2**−**OL1/OL3** and **AQ5**−**OL1/OL3**, as described above for **OL2** duplexes, reveals cleavage at the two GG steps and at G_{10} that is essentially indistinguishable from that obtained for duplexes containing **OL2** (Figure 5). Clearly, the radical cation can migrate to locations beyond the abasic site with little or no inhibition.

(6) A Trap (Low Oxidation Potential Site) on the Labeled Strand. The migration of a radical cation along the DNA might be interrupted by a trap having an oxidation potential far enough below that of its adjacent bases that insufficient energy is available for the hole to escape. In particular, for **OL2**, the proximal GG step might function as a trap that prohibits radical cations from reaching the distal sequence. It does not, as the experiments described above reveal. We prepared a specially modified oligonucleotide complementary to **OL1** to attempt to trap the radical cation.

The ideal trap for the migrating radical cation is a modified base that does not distort the structure of the duplex DNA and has an oxidation potential significantly below that of the GG step. We selected the guanine derivative 8-OxoG as the trap on this basis. Williams and co-workers recently determined the structure of a DNA duplex having an 8-OxoG substitution by X-ray crystallography and found that the oxidized base causes little perturbation.[44] And NMR spectroscopy has revealed that the replacement of G by 8-OxoG has little or no effect on global duplex structure.[45] Indeed, 8-OxoG forms Watson−Crick-type hydrogen bonds with a complementary cytosine. Foote and Sheu reported that the oxidation potential of 8-OxoG is ca. 0.4 V below that of guanosine (as their *tert*-butyldimethylsilyl-protected nucleoside derivatives).[46] Considering that the difference in oxidation potential between G and A is only ca. 0.1 V, 8-OxoG could provide a deep trap for holes migrating through the DNA strand.

We prepared **OL4**, which is identical to **OL2** except that G_{18} is replaced by an 8-OxoG. Substitution at G_{18} was selected because it is the 5′-G of the proximal GG step. The remaining GG step at positions 13,14 provides an internal control to measure the ability of the radical cation to migrate beyond the 8-OxoG position. Irradiation and analysis of **AQ2**−**OL1/OL4** was carried out as described above for the duplexes containing **OL2**. One complication in this experiment is that a small amount of strand cleavage occurs at the 8-OxoG site following piperidine treatment of unirradiated samples (Figure 6). This observation confirms a similar result reported by Cullis and co-workers.[47] Also, after 20 min of irradiation, spontaneous cleavage (no piperidine treatment required) is detected at the bases located 3′ to the 8-OxoG site, and similar to Cullis' observation, little spontaneous cleavage is detected at the 8-OxoG itself. However, most significantly, Figure 6 reveals that substitution by 8-OxoG for G_{18} greatly reduces the efficiency of light-induced cleavage at the distal GG step and at G_{19} while yielding enhanced strand cleavage at the 8-OxoG site.

Additional control experiments to assess the role of $^1O_2$ in the cleavage of **AQ2**−**OL1/OL4** were carried out since Foote and co-workers showed that 8-OxoG is ca. 100 times more reactive than is G toward this reagent.[46] Comparison of the irradiation of **AQ2**−**OL1/OL4** in H_2O with the same reaction in D_2O showed no increase in cleavage efficiency for the latter (data not shown). Significantly, the cleavage pattern obtained for a MB-initiated reaction of **AQ2**−**OL1/OL4** shows strong damage at 8-OxoG and at each of the guanines in the sequence. This reaction exhibits a pronounced H_2O/D_2O effect— clearly identifying participation by $^1O_2$ (data not shown). On the basis of these observations, radical cation migration is the cause of reaction at the remote 8-OxoG site of **AQ2**−**OL1/OL4**. Further, the damage to the DNA is concentrated at the 8-OxoG site. This finding may have important significance to the mechanisms of DNA damage and repair.

Discussion

(1) Structure of the Anthraquinone-Conjugated DNA Duplexes. The synthetic and analytical results described above leave little doubt that the gross features of the conjugated DNA duplexes are accurately represented by the structures depicted

(43) Beratan, D. N.; Priyadarshy, S.; Risser, S. M. *Chem. Biol*. **1997**, *4*, 3−8.

(44) Lipscomb, L. A.; Peek, M. E.; Morningstar, M. L.; Verghis, S. M.; Miller, E. M.; Rich, A.; Essigmann, J. M.; Williams, L. D. *Proc. Natl. Acad. Sci. U.S.A.* **1995**, *92*, 719−723.

(45) Oda, Y.; Uesugi, S.; Ikehara, M.; Nishimura, S.; Kawase, Y.; Ishikawa, H.; Inoue, H.; Ohtsuka, E. *Nucleic Acids Res*. **1991**, *19*, 1407−1412.

(46) Sheu, C.; Foote, C. S. *J. Am. Chem. Soc*. **1995**, *117*, 6439−6442.

(47) Cullis, P. M.; Malone, M. E.; Merson-Davies, L. A. *J. Am. Chem. Soc*. **1996**, *118*, 2775−2781.

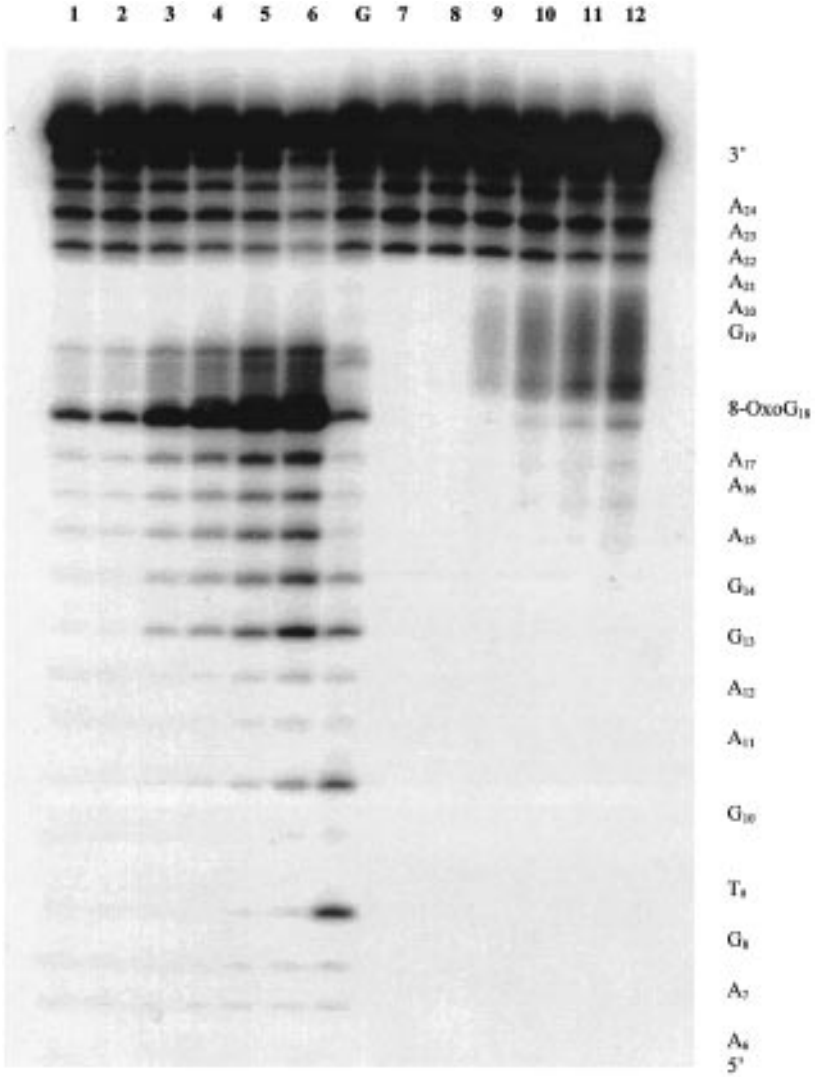

Figure 6. Autoradiogram demonstrating DNA cleavage of **OL4** in **AQ2**−**OL1/OL4** duplexes as induced by irradiation of the anthraquinone (350 nm). Samples contained 5 μM duplex DNA and 4000 cpm ^{32}P end-labeled **OL4** in 10 mM sodium phosphate buffer (pH = 7). Light control (lanes 1 and 7): 1, 40 min irradiation of **OL1/OL4** followed by piperidine treatment; 7, 40 min irradiation of **OL1/OL4** without piperidine treatment. Irradiation of **AQ2**−**OL1/OL4** duplexes: (1) piperidine-treated lanes: 2, 0 min irradiation; 3, 5 min irradiation; 4, 10 min irradiation; 5, 20 min irradiation; 6, 40 min irradiation. (2) Spontaneous lanes: 8, 0 min irradiation; 9, 5 min irradiation; 10, 10 min irradiation; 11, 20 min irradiation; 12, 40 min irradiation. Cleavage products were separated on a 20% denaturing polyacrylamide gel. Lane G is the sequencing lane.

in Chart 1. The anthraquinone group is covalently linked to the 5′-terminus, and the duplex DNA is expected to be in its stranded B-form in all cases studied.

The anthraquinone group of **AQ2**−**OL1/OL2** and **AQ5**−**OL1/OL2** must interact with the π-electron system of the DNA bases. It is possible for the quinone of **AQ5**−**OL1/OL2** to intercalate between the first base pairs of the 5′-**OL1** terminus. But **AQ2**−**OL1/OL2** cannot be intercalated; the tether is too short to permit it to assume an allowable intercalation geometry even at the first site. However, the properties of these two duplexes are essentially identical as far as we have investigated them. Their T_m values, which are the same, indicate stabilization of the duplexes by the quinone substituents. Analysis of their phosphorescence quenching behavior gives results typical of an intercalated quinone that is largely independent of the linking chain length. Their irradiation gives DNA strand cleavage that is characteristic of electron transfer and is also independent of the tether length. But, unlike **AQC**, the photoinduced cleavage is quenched by dAMP.

These findings suggest that neither the anthraquinone group of **AQ2**−**OL1/OL2** or **AQ5**−**OL1/OL2** is intercalated in the DNA. However, the T_m data and the phosphorescence quenching results both clearly reveal a close interaction of the quinone and DNA. These observations lead us to suggest that these anthraquinones are "end-capping" the DNA. In this mode of association, the quinone is stacked against the last base pair in the duplex DNA structure. A model for such a structure is presented in Figure 7.

The driving forces for end-capping are similar to those for intercalation.[48] The hydrophobic anthraquinone group is partially shielded from the aqueous solvent, and an electron donor (a DNA base)−electron acceptor (the quinone) interaction in addition to $\pi-\pi$ interactions serves to lower the free energy of the system.[49] An end-capped structure accommodates the similarity in behavior seen for **AQ5**−**OL1/OL2** and **AQ2**−**OL1/OL2**. It permits the rapid reaction of the excited state demanded by the phosphorescence results while permitting access to the quinone by negatively charged quenchers. Deduction of a structure from chemical and spectroscopic observations is necessarily speculative. For this reason we are currently

(48) Lerman, L. S. *Proc. Natl. Acad. Sci. U.S.A.* **1963**, *49*, 94.
(49) Guckian, K. M.; Schweitzer, B. A.; Ren, R., X-F.; Sheils, C. J.; Paris, P. L.; Tahmassebi, D. C.; Kool, E. T. *J. Am. Chem. Soc.* **1996**, *118*, 8182−8183.

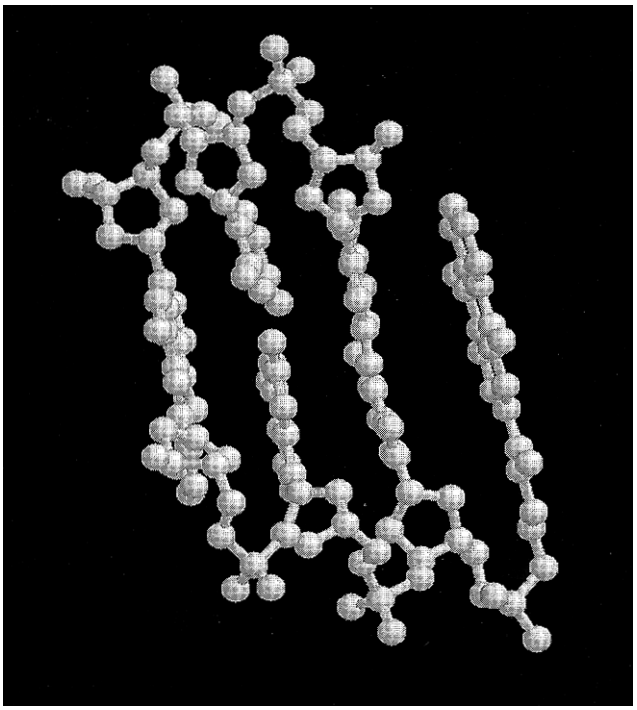

Figure 7. Model illustrating end-capping of the DNA duplex by covalently attached anthraquinone. The covalent linkage is identical to that in **AQ2**−**OL1**. The DNA coordinates used in this model were downloaded from the Protein Data Bank.[53] The three base pairs shown were removed from the end (sequence 5′-CGC-3′). The model structure was created in Biosym by creating a bond between the anthraquinone and the 5′-OH of the DNA followed by manipulation of the linker torsion angles to place the anthraquinone over the CG base pair.

attempting to crystallize analogues of the linked duplexes for X-ray analysis. Nevertheless, the circumstantial support for the end-capped structure is strong, and it permits a consistent interpretation of the results.

(2) Long-Range Damage at Guanine. The migration of a hole or electron in duplex DNA from its point of generation to a site of reaction has been invoked to explain several experimental observations.[21,50,22] In most cases, the reaction site is clearly defined but the generation site is difficult to determine with certainty. This problem can be solved with the conjugated duplex structures described herein and the similarly-linked compounds described by Barton and co-workers.[26] In the anthraquinone-linked compounds, the point of radical cation generation is known with some certainty because of structural constraints, and the site of reaction is revealed clearly by strand cleavage. These results, therefore, verify migration of the radical cation through the duplex DNA and permit examination of the effect of perturbations to the migration route.

Three perturbations to the migration route were investigated. The first explores the effect of the proximal GG step on migration to the distal GG step. The results show that there is no effect. Both GG steps are cleaved with the same efficiency. It is important to remember that the efficiency (quantum yield) of a reaction is determined by a ratio of rates. In the current case, this ratio involves the rate of irreversible reaction of the G radical cation with an external reagent (H_2O or O_2) compared with the rate for escape of the hole from the GG trap. The results require that the latter be significantly larger than the former. For any other circumstance, cleavage at the proximal GG step would be more efficient than at the distal. This requirement does not shed light on the absolute rate constants for reaction or migration except as these can be estimated rom theory or additional experiment. Since theory cannot yet yield a definitive answer,[43] we are pursuing experiments to measure relative and absolute rate constants for hole migration.

The second perturbation of the migration route examined is the introduction of an abasic site in **OL3**. Cuniasse and co-workers have analyzed duplex DNA with T, C, and G bases opposite an abasic site by NMR spectroscopy.[51] They find for T opposite the abasic site, as is the case for **AQ2**−**OL1/OL3**, that at ca. 30 °C about one-half of the structures have an intrahelical base that preserves a gap in the basic strand. For the fraction of structures that have an extrahelical T, the abasic strand can collapse around the gap and may reestablish some π-electron overlap between adjacent bases. Our experiments reveal that neither the gap nor the extrahelical T on the opposite strand inhibits the migration of the radical cation to the distal GG step of the **OL1** strand.

This finding has two likely explanations. First, it is not certain that the gap introduced by the abasic site will reduce the π-electron overlap sufficiently to slow the rate of hole migration enough to allow irreversible reaction at the GG step to have the significantly greater rate. Distortion of the DNA structure adjacent to the abasic site may reposition the bases to exclude water. This reorganization can reduce the average distance between the surrounding bases and thus maintain π-electron overlap. Precisely the same reasoning may be invoked to explain hole migration that is more rapid than trapping when the opposing T is extrahelical.

Alternatively, the radical cation may migrate past the abasic site *via* the opposite strand of the duplex. The end-capped model proposed for the structure of these conjugates does not specify initial generation of the radical cation in the linked or labeled strand. It is certainly possible that the rate of hole migration from one strand to its complement is faster than the irreversible reaction of the radical cation at a GG step. Whatever the mechanism, clearly, neither a GG step or an abasic site presents a significant barrier to radical cation migration in duplex DNA.

(3) 8-OxoG: A Trap of Sufficient Depth. Substitution of 8-OxoG at G_{18} in **AQ2**−**OL1/OL4** introduces a low oxidation potential site in the DNA without distorting the structure of the duplex. The irradiation of this compound shows some spontaneous cleavage at bases 3′ to the 8-OxoG (none is seen for the unmodified duplexes) and, most importantly, cleavage at G_{10}, G_{13}, G_{14}, and at G_{19} is essentially completely inhibited. Further, the efficiency of damage at the 8-OxoG site is greater than is seen for any site in the unmodified duplex. These observations provide insight into the migration of the radical cation in duplex DNA and into the reactivity of damaged bases.

Cullis and co-workers carried out experiments to define the G-oxidation product responsible for cleavage of DNA.[47] By comparison of the rates of cleavage for authentic 8-OxoG-containing oligonucleotides with those containing an oxidatively-damaged guanine, they conclude that 8-OxoG is not the primary species responsible for piperidine-dependent cleavage. Our findings reveal that 8-OxoG is the preferred site for localization and reaction of a radical cation in duplex DNA. And, as Cullis also notes, the oxidized 8-OxoG is more sensitive to piperidine-induced cleavage than is 8-OxoG itself.

The enhanced and nearly exclusive cleavage of **AQ2**−**OL1/OL4** at 8-OxoG may be due either to localization of the radical cation at this low oxidation potential site or to an acceleration

(50) Hall, D. B.; Barton, J. K. *J. Am. Chem. Soc.* **1997**, *119*, 5045−5046.

(51) Cuniasse, P.; Fazakerley, G. V.; Guschlbauer, W.; Kaplan, B. E.; Sowers, L. C. *J. Mol. Biol.* **1990**, *213*, 303−314.

of the rate of irreversible reaction of the 8-OxoG radical cation with H_2O or O_2. The former seems far more likely since the bimolecular reaction rate of the radical cation with H_2O or O_2 cannot exceed an encounter rate which is limited by access to the hydrophobic interior of the DNA. Whatever the cause, it is clear that 8-OxoG is a trap for the migrating radical cation and this prevents damage at the distal GG step in **AQ2**−**OL1/OL4**. This finding has potential significance to mutagenesis since radical cations migrating in DNA will "accumulate" at guanines, particularly GG steps, yielding damage that is associated with mutations.[10]

(4) Mechanism of Long-Distance Guanine Damage. The findings presented herein leave no doubt that a radical cation introduced near the 3′-terminus of duplex DNA can oxidize a guanine more than 40 Å away. Two limiting models for this hole migration have been considered.[43] The first is electron tunneling through a series of hops by a hole localized on one base (trap) to an adjacent base until the hole is consumed by a reaction or it falls into a trap too deep to escape. The second mechanism for migration occurs when the electronic coupling between the basis is so strong that they may be considered to be like a semiconductor with the hole delocalized over all bases simultaneously. Our findings can be accommodated by either limiting mechanism. If the hole hops, the depth of each trap will control the escape rate. The hole will spend more time at the deeper traps (GG steps, 8-OxoG), and irreversible reaction there will be more likely. If the hole is delocalized, its density at low oxidation potential sites will be higher and irreversible reaction is again more likely.

Our findings show that the hole migration process is not easily disturbed. Neither the proximal GG step nor the abasic site interrupts the migration enough to modify the distribution of G-damage sites. These results stand in contrast to findings reported recently by Hall and Barton where it appears that a single-strand bulge inhibits oxidative damage at a distal GG site.[50] This finding is attributed to perturbation of long-range hole migration, but it may also be a consequence of the distortion of the DNA structure by the nearby single-stranded region. Whatever the explanation, on the basis of the findings reported herein, it is probably premature to conclude that comparing cleavage at proximal and distal GG step is a reliable method for characterizing the continuity of the π-stack in duplex DNA.[50]

Experimental Section

General Procedure. ^{1}H and ^{13}C NMR spectra were recorded on a Varian 300 MHz spectrometer. ^{31}P NMR were recorded on a Bruker 400 MHz spectrometer. Methylene chloride was dried over CaH_2 and distilled. Diisopropylethylamine, *N*,*N*-diisopropylmethylphosphonamidic chloride, thionyl chloride, 2-aminoethanol, and 5-aminopentanol were purchased from Aldrich and used without further purification. Anthraquinone-2-carboxylic acid was purchased from TCI and used without further purification. **AQC** was synthesized as previously described.[11] Unmodified oligonucleotides (gel filtration grade) were obtained from the Midland Certified Reagent Co. Anthraquinone-modified oligonucleotides were synthesized on a Applied Biosystems DNA synthesizer and were purified by HPLC. dAMP·Na_2 was obtained from Sigma. Unmodified oligonucleotide solution concentrations were determined by the absorbance at 260 nm. Anthraquinone-modified oligonucleotide solution concentrations were determined using the absorbance of the anthraquinone at 334 nm. Ion exchange HPLC was performed on a Hitachi system using a Vydac column. The buffer solution used in all DNA experiments was 0.1 M sodium phosphate.[52] UV melting and cooling curves were recorded on a Cary 1E spectrophotometer equipped with a multicell block, temperature controller and sample transport accessory. Phosphorescence emission spectra were measured on a Spex Fluorolog spectrofluorimeter. Histograms from autoradiograms were obtained using UTHSCSA Image Tool Version 1.27 in conjunction with a HP ScanJet IIcx scanner.

***N*-(2-Hydroxyethyl)-2-anthraquinonecarboxamide.** A solution of 687 mg (2.5 mmol) of anthraquinone-2-carbonyl chloride in 20 mL of dry methylene chloride was added dropwise to a solution of 0.61 mL (10 mmol) of 2-aminoethanol and 0.37 (2.7 mmol) of triethylamine in 90 mL of dry methylene chloride. The mixture, which became cloudy upon complete addition of the antraquinone-2-carbonyl chloride solution, was stirred overnight at room temperature. The solution was filtered and a pale yellow solid was isolated. Recrystallization from hot isopropyl alcohol gave 545 mg (73%) of *N*-(2-hydroxyethyl)-2-anthraquinonecarboxamide (mp 199−200 °C): ^{1}H NMR (300 MHz, DMSO-d_6) δ 3.40 (t, 2H, methylene), 3.56 (t, 2H, methylene), 4.80 (t, 1H, hydroxyl), 7.90−7.93 (m, 2H, aromatic), 8.16−8.33 (m, 4H, aromatic), 8.61 (d, J = 1.56 Hz, 1H, aromatic), 8.92 (t, 1H, amide); ^{13}C NMR (300 MHz, DMSO-d_6) δ 42.46, 59.58, 125.70, 126.93, 126.97, 127.15, 132.96, 133.17, 133.21, 134.61, 134.80, 139.57, 164.94, 182.35, 182.37; HRMS (CI) *m*/*z* 296.0927 (296.0923, calcd for $C_{17}H_{13}NO_4 + H^+$).

***N*-(5-Hydroxypentyl)-2-anthraquinonecarboxamide.** A solution of 687 mg (2.5 mmol) of anthraquinone-2-carbonyl chloride in 20 mL of dry methylene chloride was added dropwise to a solution of 1.12 mL (10 mmol) of 5-amino-1-pentanol and 0.37 mL (2.7 mmol) of triethylamine in 90 mL of dry methylene chloride. The mixture, which became cloudy upon complete addition of the anthraquinone-2-carbonyl chloride solution, was stirred overnight at room temperature. The solution was filtered, and a pale yellow solid was isolated. Recrystallization from hot isopropyl alcohol gave 468 mg (55%) of *N*-(5-hydroxypentyl)-2-anthraquinonecarboxamide (mp 132−133 °C): ^{1}H NMR (300 MHz, DMSO-d_6) δ 1.32−1.61 (m, 6H, methylene), 3.30 (q, 2H, methylene), 3.41 (t, 2H, methylene), 7.87−7.93 (m, 2H, aromatic), 8.14−8.30 (m, 4H, aromatic), 8.58 (d, J = 1.3 Hz, 1H, aromatic), 8.91 (t, 1H, amide); ^{13}C NMR (300 MHz, DMSO-d_6) δ 23.04, 28.83, 32.22, 60.65, 125.60, 126.92, 126.96, 127.13, 132.92, 133.15, 133.18, 133.23, 134.58, 134.77, 139.66, 165.66, 185.33, 182.35; HRMS (CI) *m*/*z* 338.1406 (338.1392, calcd for $C_{20}H_{19}NO_4 + H^+$).

***N*-(2-(Methoxy(diisopropylamino)phosphinyl)ethyl)-2-anthraquinonecarboxamide.** *N*-(2-Hydroxyethyl)-2-anthraquinonecarboxamide (259 mg, 0.878 mmol) was suspended in a solution of 0.67 mL of *N*,*N*-diisopropylethylamine in 2.0 mL of dry methylene chloride. With stirring, 0.17 mL (0.88 mmol) of *N*,*N*-diisopropylmethylphosphonamidic chloride was added dropwise. Upon complete addition, a clear orange-red solution was obtained which was stirred at room temperature for 30 min. The mixture was poured into 5 mL of ethyl acetate containing 0.5 mL of triethylamine. The organic layer was washed two times with 5 mL of 5% sodium bicarbonate and two times with 5 mL of brine and dried over sodium sulfate. The solvent was removed *in vacuo* to give 504 mg of a thick, dark red oil which was purified by column chromatography on silica gel using a 45:45:10 ethyl acetate:hexane:triethylamine eluent. Combined fractions gave 257 mg (64%) of a thick, dark red oil: ^{1}H NMR (300 MHz, $CDCl_3$) δ 1.19 (d of d, J = 5.0 Hz and 1.8 Hz, 14H, methyl), 3.46 (d, J = 13 Hz, 3H, methoxy), 3.58−3.76 (m, 5H, methine and methylene), 3.88−3.94 (m, 2H, methylene), 7.37 (br. t, 1H, amide), 7.81−7.84 (m, 2H, aromatic), 8.30−8.41 (m, 4H, aromatic), 8.64 (d, J = 1.5, 1H, aromatic); ^{31}P NMR (162 MHz, CD_3CN) δ 149.89.

***N*-(5-(Methoxy(diisopropylamino)phosphinyl)pentyl)-2-anthraquinonecarboxamide.** *N*-(5-Hydroxypentyl)-2-anthraquinonecarboxamide (194 mg, 5.6 mmol) was suspended in a solution of 0.44 mL of *N*,*N*-diisopropylethylamine in 1.5 mL of dry methylene chloride. With stirring, 0.11 mL (5.7 mmol) of *N*,*N*-diisopropylmethylphosphonamidic chloride was added dropwise. Upon complete addition, a clear orange-red solution was obtained which was stirred at room temperature for 30 min. The mixture was poured into 5 mL of ethyl acetate containing 0.5 mL of triethylamine. The organic layer was washed two times with 5 mL of 5% sodium bicarbonate and two times with 5 mL of brine and dried over sodium sulfate. The solvent was removed *in vacuo* to give 340 mg (118%) of a thick, dark red oil (We were

(52) Sambrook, J.; Fritsch, E. F.; Maniatis, T. *Molecular Cloning. A Laboratory Manual*, 2nd ed.; Cold Spring Harbor Press: Cold Spring Harbor, NY, 1989.

(53) Brown, T.; Hunter, W. N.; Kneale, G.; Kennard, O. *Proc. Natl. Acad. Sci. U.S.A.* **1986**, *83*, 2402.

unable to completely purify this material by column chromatography. The ^{1}H NMR contains several impurities which appear to be residual solvent. These may account for the high yield and for the high integration observed for the methyl, methylene, and methine regions.): ^{1}H NMR (300 MHz, $CDCl_3$) δ 1.16 (d, J = 6.3 Hz, 17H, methyl), 1.22−1.25 (m, 8H, methylene), 3.38 (d, J = 13.3 Hz, 4H, methoxy), 3.48−3.64 (m, 8H, methylene and methine), 6.57 (br. t, 1H, amide), 7.80−7.83 (m, 2H, aromatic), 8.26−8.38 (m, 4H, aromatic), 8.55 (d, J = 1.80 Hz, 1H, aromatic); ^{31}P NMR (162 MHz, CD_3CN) δ 148.084.

UV Melting. A 2.5 μM solution of the appropriate oligonucleotides in 10 mM phosphate buffer, pH = 7, was prepared. Melting curves were obtained by monitoring the absorbance at 260 nm as the temperature was ramped from 65 to 20 °C at a rate of 0.5 deg/min. Data obtained for cooling were found to be the same as those obtained from heating.

Phosphorescence Quenching. Solutions of the appropriate oligonucleotides in 10 mM phosphate buffer were hybridized and diluted with ethylene glycol to a final concentration of 10 μM. Final solutions containing 33% ethylene glycol and 10 mM phosphate were transferred to NMR tubes which were submerged in liquid nitrogen contained in an optical Dewar flask. The samples were excited at 330 nm, and the phosphorescence emission spectra were recorded from 400−600 nm.

Cleavage Analysis by Radiolabeling and PAGE. Either OL2, OL3, or OL4 was radiolabeled at the 5′-OH using [γ-^{32}P]ATP and bacterial T4 Polynucleotide kinase.[52] Radiolabeled DNA was purified by 20% PAGE. Samples for irradiation were prepared by hybridizing a mixture of cold and radiolabeled oligonucleotide (5 μM) with 5 μM of either **OL1**, **AQ2**−**OL1**, or **AQ5**−**OL1** in phosphate buffer. Hybridization was achieved by heating the samples at 80 °C for 5 min and slowly cooling to room temperature. These samples were irradiated in microcentrifuge tubes in a Rayonet photoreactor containing 8 × 350 nm lamps. After irradiation, the samples were precipitated once and then treated with hot piperidine for 30 min.[52] Samples (1000 cpm) were electrophoresed on a 20% denaturing 19:1 acrylamides:bisacrylamide gel containing 7 M urea. Gels were dried and the cleavage visualized by autoradiography.

Methylene Blue Cleavage and Cleavage in H_2O/D_2O. Samples of the oligonucleotides were prepared as described above and were then concentrated to dryness. H_2O or D_2O was added, and the samples were hybridized. Prior to irradiation, methylene blue was added to a concentration of 10 μM. A 150 W Hg−Xe lamp with a 600 nm cutoff filter was used for irradiation of methylene blue-containing samples. After irradiation, the samples were precipitated, treated with piperidine, and analyzed by PAGE.

dAMP Quenching Experiments. dAMP·Na_2 was obtained from Sigma. Samples were prepared as above in 10 mM phosphate containing either 200 mM $NaClO_4$ or 100 mM dAMP (100 mM Na^+) for the linked duplexes. **AQC** samples contained 20 μM **AQC** and 5 μM duplex DNA in 10 mM phosphate with either 100 mM $NaClO_4$ or 50 mM dAMP (100 mM Na^+). Irradiation, electrophoresis, and autoradiography were performed as described above. Lanes were scanned and using Image Tool, and intensities of the cleavage bands were measured three times, averaged, and used to calculate the average I_0/I.

Acknowledgment. We thank Dr. Nadia Boguslavsky for performing the anthraquinone−oligonucleotide conjugate synthesis and purification, Dr. Les Gelbaum for help with ^{31}P NMR, and Danith Ly for help with ion exchange HPLC. This work was supported by a grant from NIH, for which we are grateful.

JA972496Z